# Supporting Information

## Carbonate deprotonation on Ni-rich layered cathode: Development of a new cis isomerism oligomer as an organic coverage

Laurien Merinda,[a] Fu-Ming Wang, *[a,b,c,d] Nae-Lih Wu,*[e] Rio Akbar Yuwono,[a] Chusnul Khotimah,[a] Ulya Qonita,[a] Wei-Hsiang Huang,[f] Lester Pei-Wan Tiong,[a] Ching-Kai Chang,[a] Ping-Hsuan Hsu,[a] Chih-Wen Pao,[f] Jeng-Lung Chen,[f] Chi-Liang Chen,[f] and Ting-Shang Chan.[f]

[a] Graduate Institute of Applied Science and Technology, National Taiwan University of Science and Technology, Taipei 10607, Taiwan.
[b] Graduate Institute of Energy and Sustainability Technology, National Taiwan University of Science and Technology, Taipei 10607, Taiwan.
[c] Department of Chemical Engineering, Chung Yuan Christian University, Taoyuan 320314, Taiwan.
[d] R&D Center for Membrane Technology, Chung Yuan Christian University, Taoyuan 320314, Taiwan.
[e] Department of Chemical Engineering, National Taiwan University, Taipei 10617, Taiwan.
[f] National Synchrotron Radiation Research Center, Hsinchu 30076, Taiwan.

*Corresponding author:

Prof. Fu-Ming Wang

IB-606, No.43, Section 4, Keelung Road, Taipei 106, Taiwan, R.O.C

E-mail: mccabe@mail.ntust.edu.tw

Tel: +886-2-27303755

Fax: +886-2-27376922

Prof. Nae-Lih Wu

Department of Chemical Engineering 208A, No.1, Section 4, Roosevelt Road, Taipei 106, Taiwan, R.O.C

E-mail: nlw001@ntu.edu.tw

Tel: +886-2-23627158

Fax: +886-2-23623040

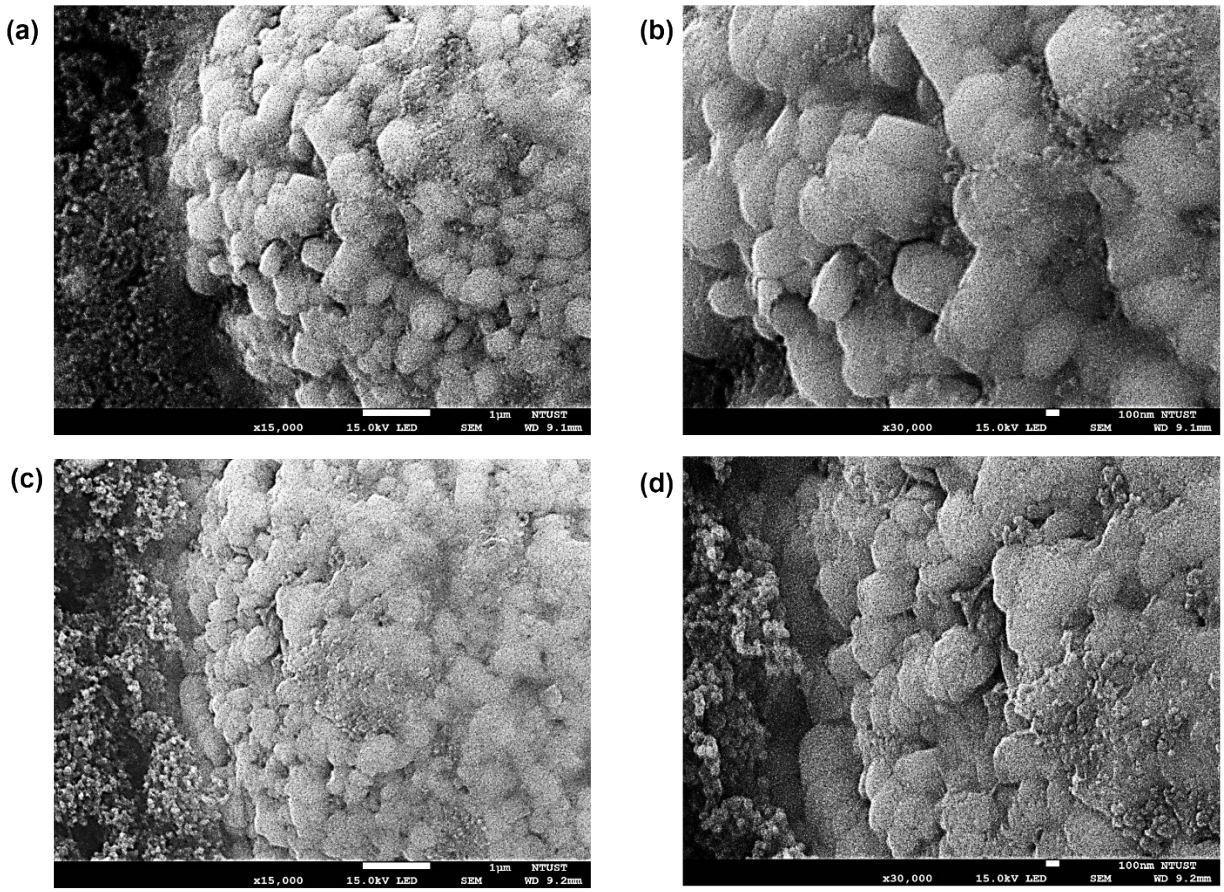


**Fig. S1** SEM images of (a, b) pristine NCM811 and (c, d) CI@NCM811 particles before cycle.

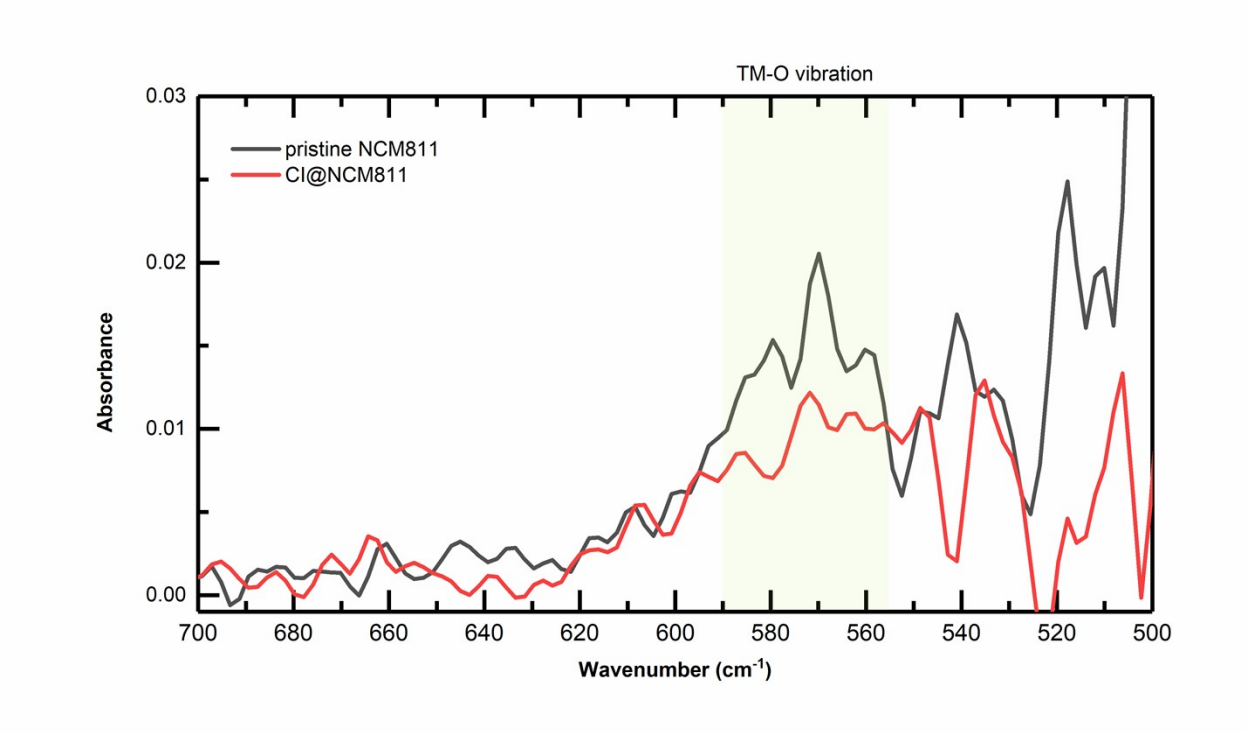


**Fig. S2** Ex situ ATR-FTIR of pristine NCM811 and CI@NCM811 before cycle.

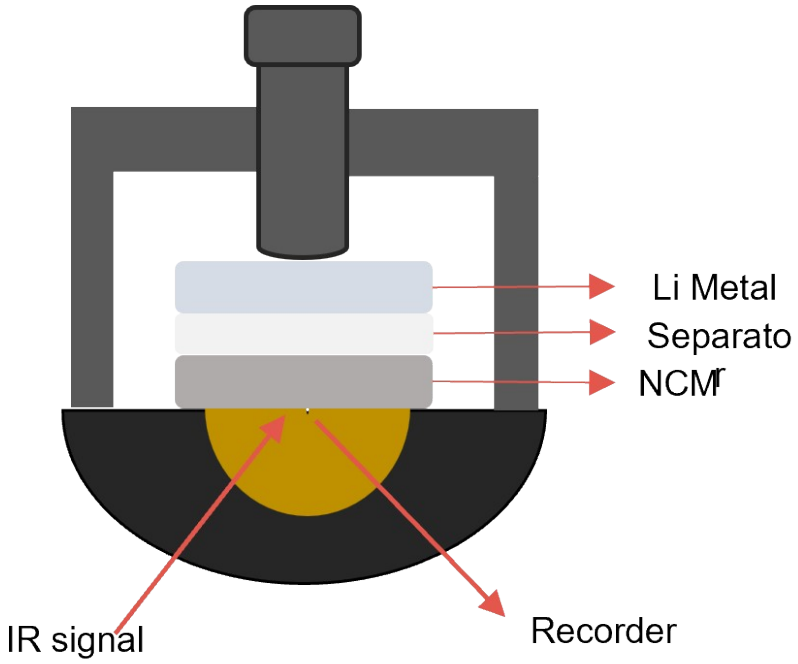


**Fig. S3** The operando ATR-FTIR electrochemical cell illustration.

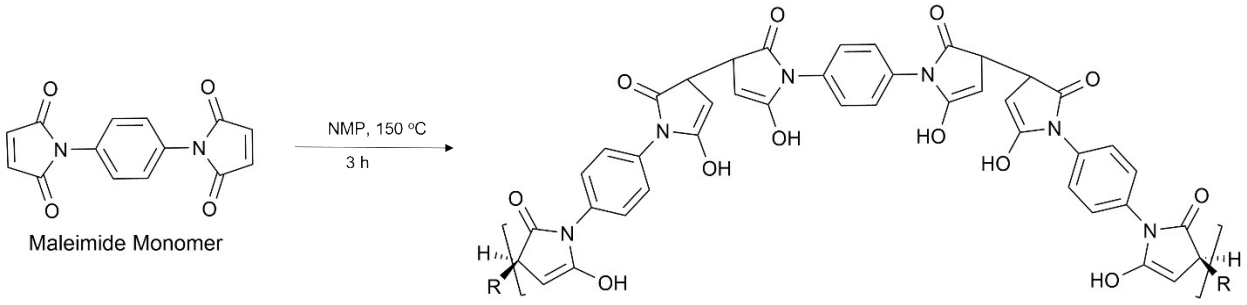


**Fig. S4** Proposed structure cis formulations of oligomer.

| | Maleimide dissolved in NMP | CI Oligomer |
|---|---|---|
| $\bar{M}n$ | 511 | 907 |
| $\bar{M}w$ | 554 | 2290 |
| PDI | $\frac{\bar{M}w}{\bar{M}n}$ = 1.08 | $\frac{\bar{M}w}{\bar{M}n}$ = 2.52 |
| $D_p$ | $\frac{\bar{M}n}{MW} = \frac{511}{268.22} = 1.9$ | $\frac{\bar{M}n}{MW} = \frac{907}{268.22} = 3.38$ |

**Table S1.** GPC characteristics of maleimide monomer in NMP and its derivative CI oligomer.

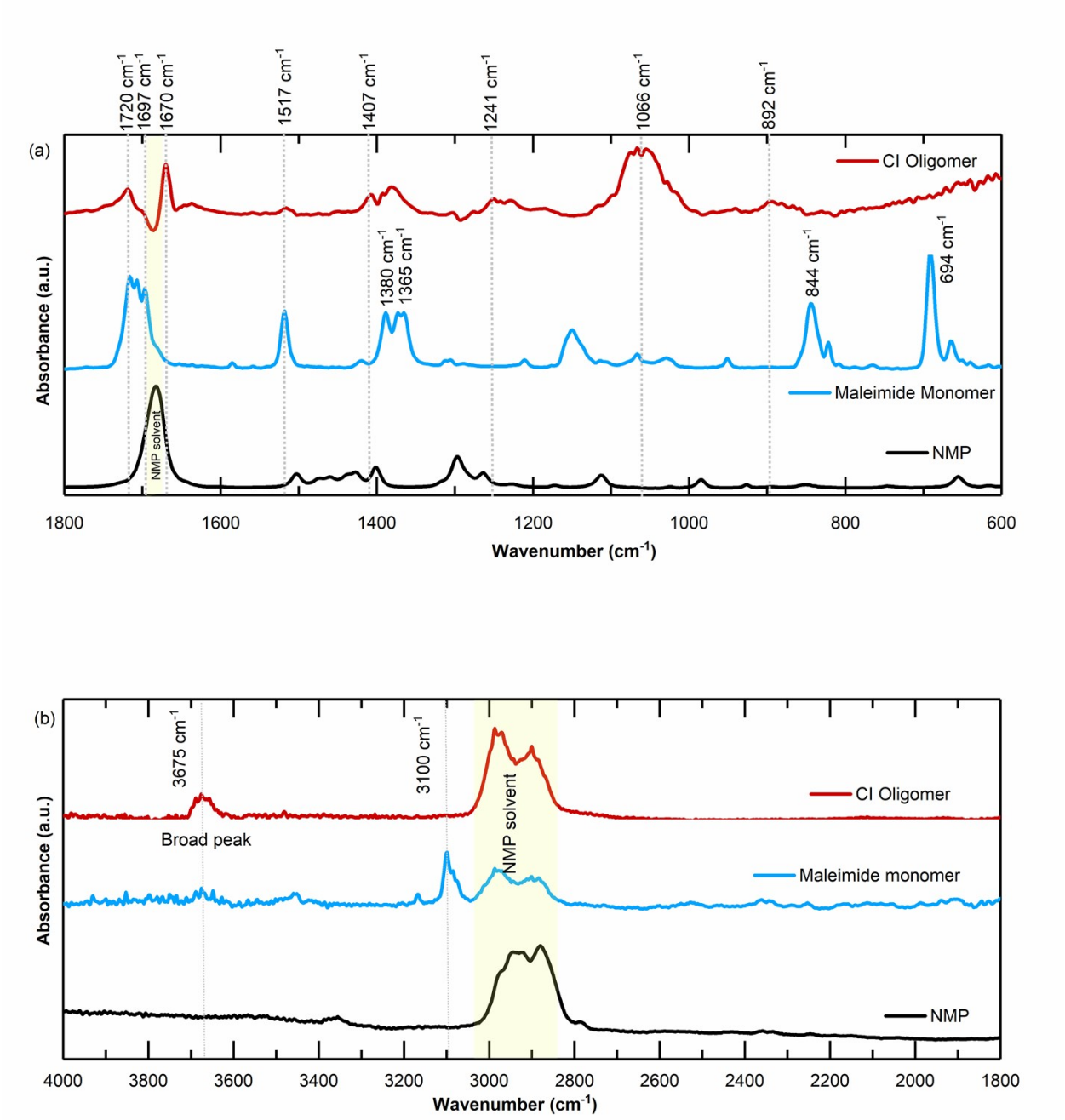


**Fig. S5** FTIR spectra of NMP, maleimide monomer, and CI oligomer at wavenumber range of (a) 600-1800 $cm^{-1}$ and (b) 1800-4000 $cm^{-1}$. The corresponding functional group for each absorption peak in certain wavenumber is mentioned in table S2.

**Table S2.** FTIR peak table of Maleimide monomer and CI oligomer (Ref. 35)

| Wavenumber ($cm^{-1}$) | Vibrational mode | Species of origin |
|---|---|---|
| 694 | C-H bending | Maleimide Monomer |
| 844 | C-H ( 1,4 – Disubstitution)/ Para | Maleimide Monomer |
| 892 | C-H ( 1,4 – Disubstitution)/ Para | CI Oligomer |
| **1066** | **C-O stretching** | **CI Oligomer** |
| 1241 | C-N stretch | CI Oligomer |
| 1365 | C-N strecth | Maleimide Monomer |
| 1380 | C-N strecth | Maleimide Monomer |
| 1407 | O-H bending | CI Oligomer |
| 1517 | Aromatic ring ( C=C-C) | Maleimide Monomer |
| **1670** | **C=C stretching** | **CI Oligomer** |
| **1697** | **C=C stretching** | **Maleimide Monomer** |
| 1720 | C=O stretching | Maleimide Monomer, CI Oligomer |
| 3100 | C=CH / C-H stretch | Maleimide Monomer |
| 3675 | -COH / -OH | CI Oligomer |

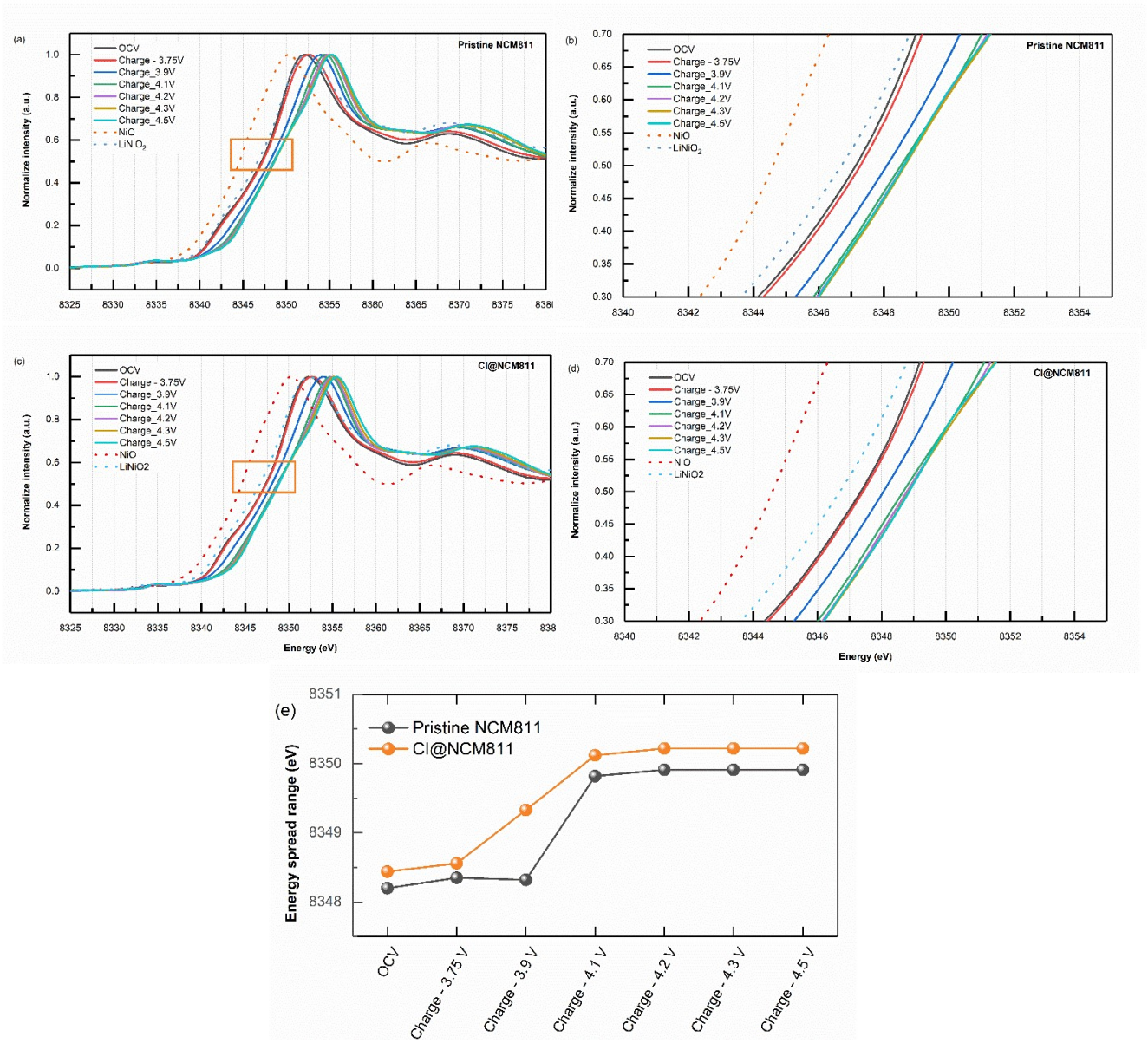


**Fig. S6** XANES spectra of Ni K-edge during first charge of (a) pristine NCM811 and (b) the magnification of the orange-square-lined region as well as (c) CI@NCM811 and (d) the magnification of the orange-square-lined region. (e) Corresponding binding energy at specify normalized intensity of 0.6 of the edge jump.

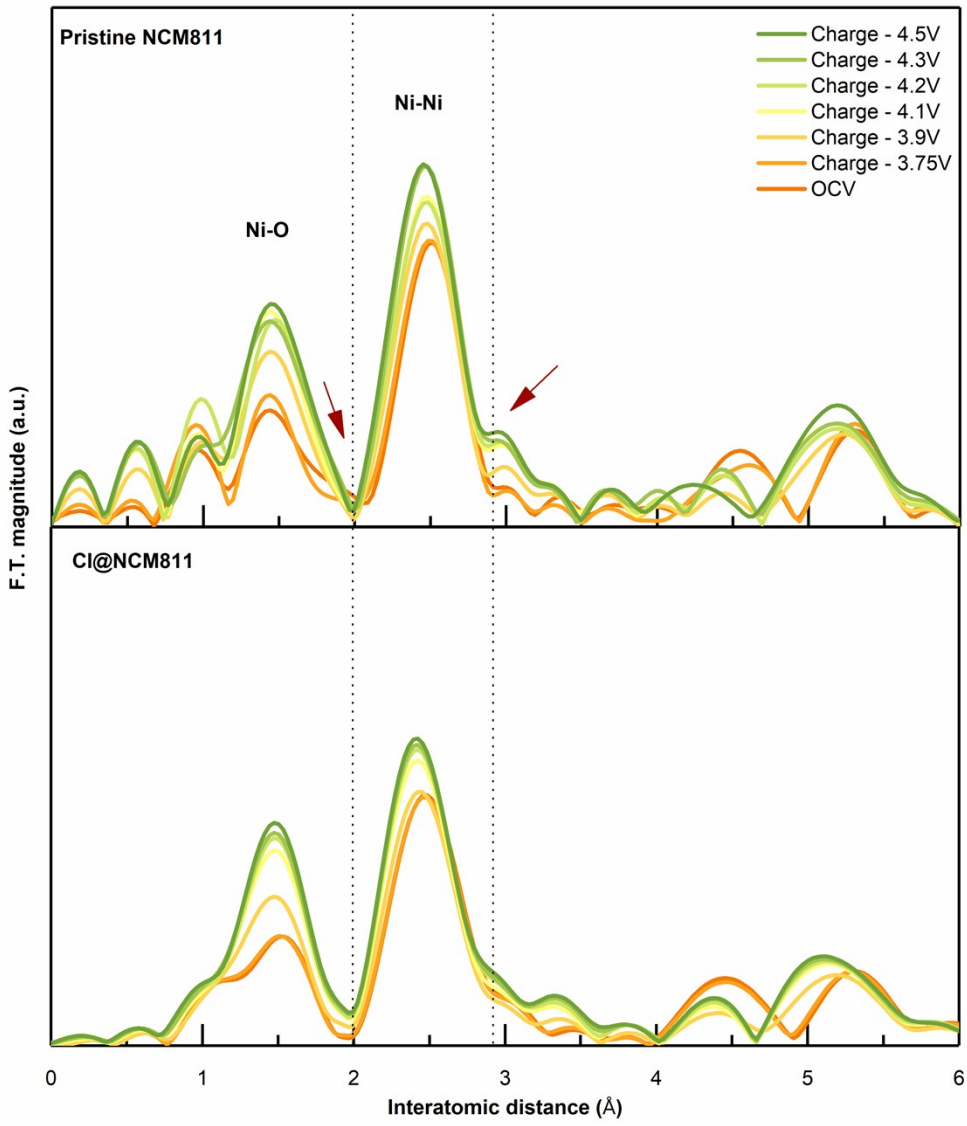


**Fig. S7** Ni K-edge EXAFS spectra of pristine NCM811 and CI@NCM811 in the first charge.

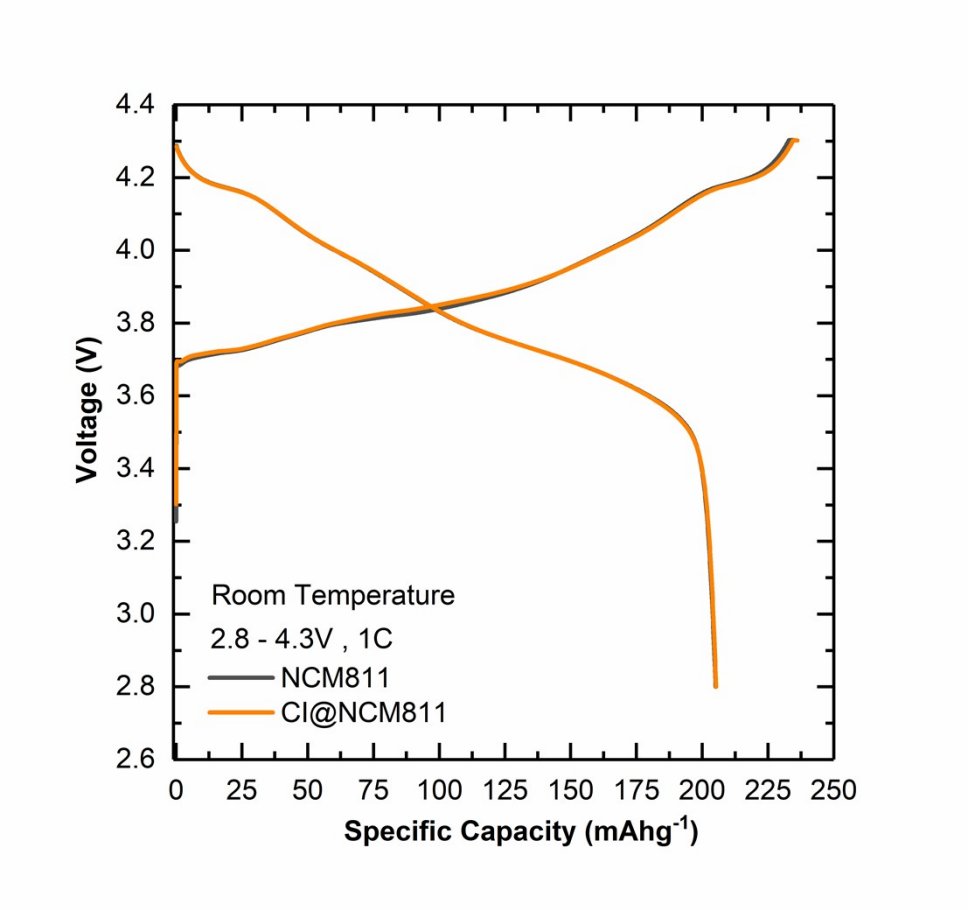


**Fig. S8** Initial voltage profile of NCM811 vs. CI@NCM811 in the half-cell configuration

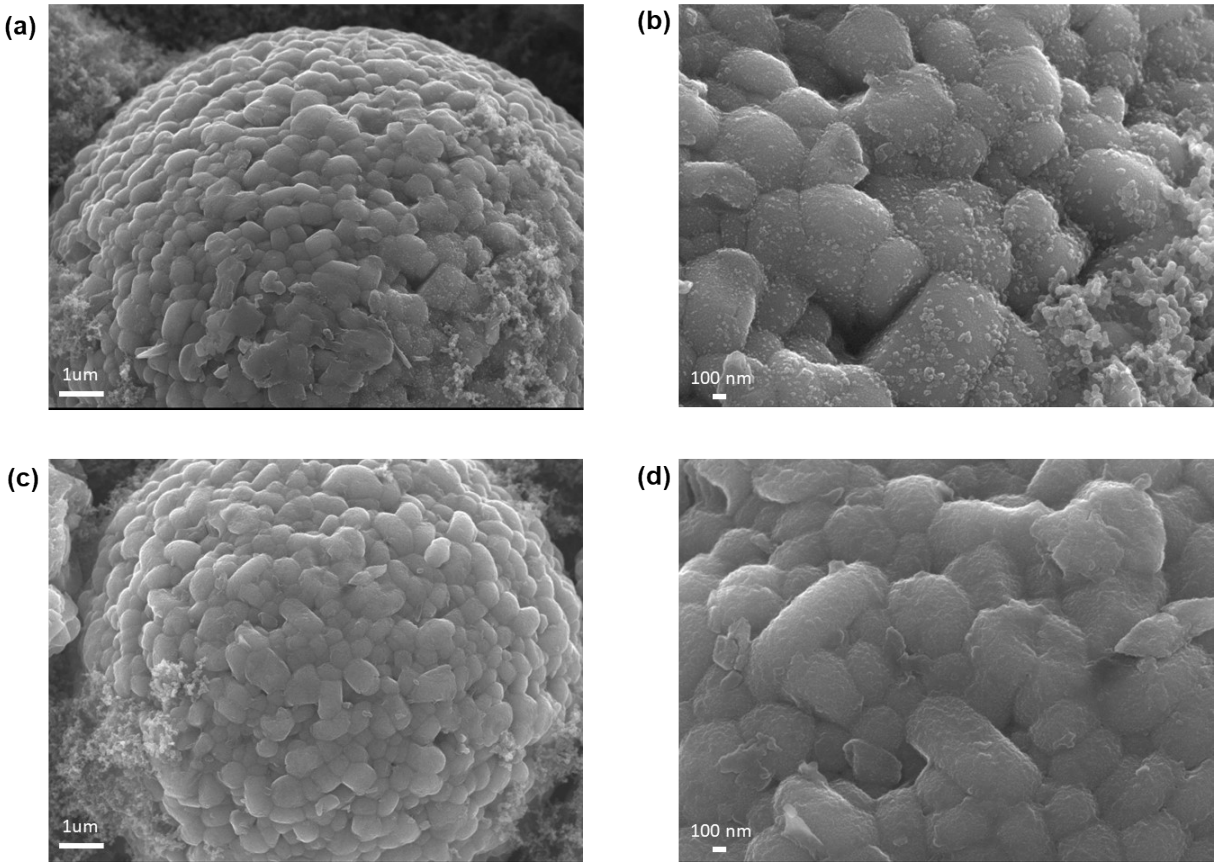


**Fig. S9** SEM images of (a, b) pristine NCM811 and (c, d) CI@NCM811 electrode after cycling in half cell configuration.

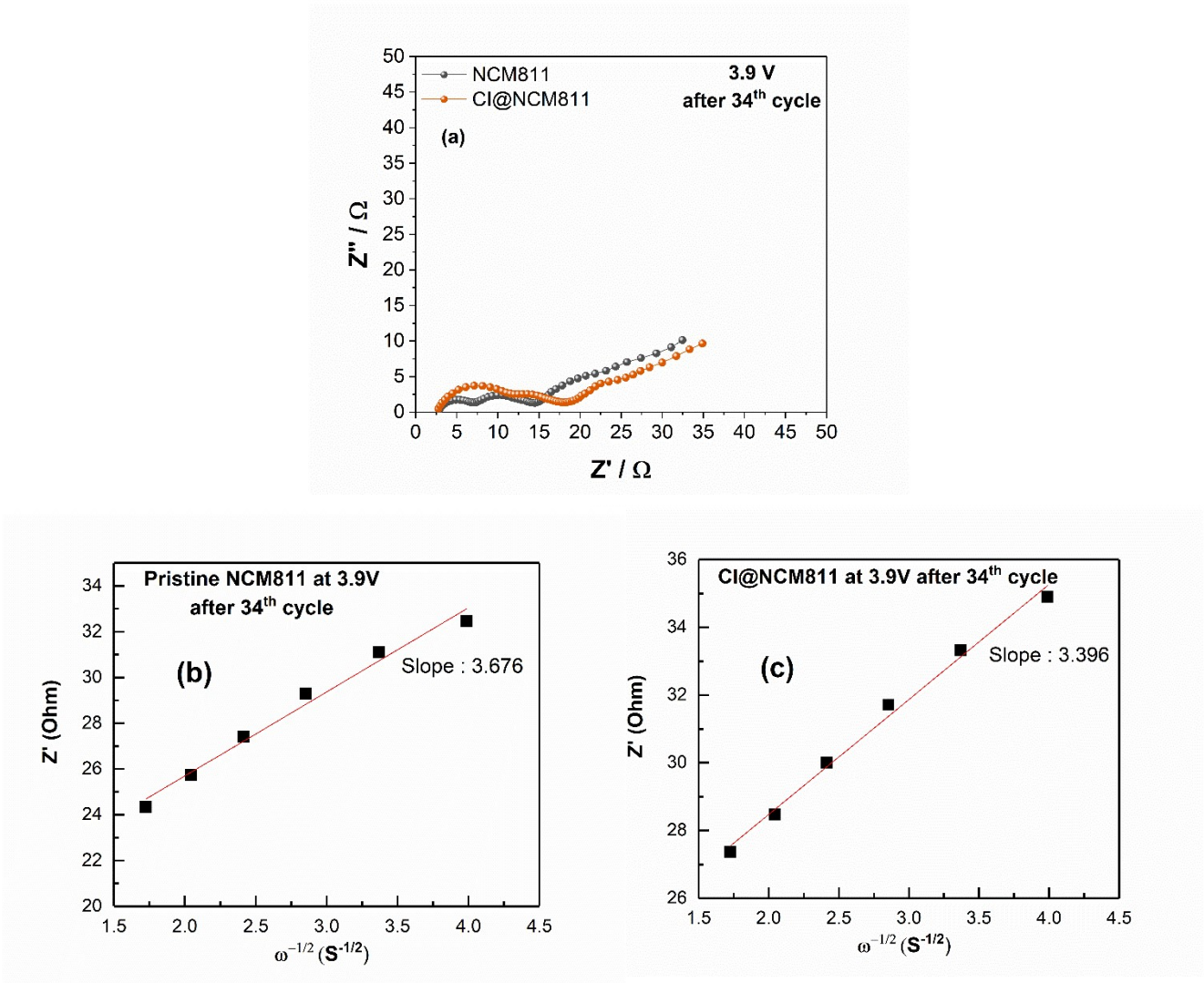


**Fig. S10** The Nyquist plot of pristine NCM811 and CI@NCM811 after 34th cycle at charge state 3.9 V **(a)**. The linear slope of $Z_w$ and $\omega^{-1/2}$ *at low frequency for* pristine NCM811 **(b)** and CI@NCM811 **(c)** after 34th cycle at charge state 3.9 V.

The semi-circles of the two electrodes in high-frequency region representing the electrolyte resistance, cathode-electrolyte interface resistance and charge transfer resistance. Low freq tail was attributed to the Warburg impedance ($Z_w$) of $Li^+$ diffusion in the cathode material. [1]

The diffusion coefficient value can be obtained by the following equation (1): [2–4]

$$D_{Li^+} = 0.5\left(\frac{RT}{A\,F^2\sigma_\omega C}\right)^2 \qquad (1)$$

Where R represents the gas constant, T is the Kelvin temperature, A is the total surface of the electrode, F is Faraday's constant, $\sigma_\omega$ is the linear slope between Warburg impedance ($Z_w$) and frequency region ($\omega^{-1/2}$) and C is the molar concentration of lithium in the active material.

The $Li^+$ diffusion coefficient calculated by eq 1 of pristine NCM811 and CI@NCM811 after prolonged cycle condition are 3.82 x $10^{-8}$ $cm^{-2}$ $s^{-1}$ and 4.48 x $10^{-8}$ $cm^{-2}$ $s^{-1}$, respectively. This value were similar to previous report that stated the $D_{Li+}$ in the charge process are between $10^{-8}$ to $10^{-9}$ $cm^{-2}$ $s^{-1}$.[5,6]

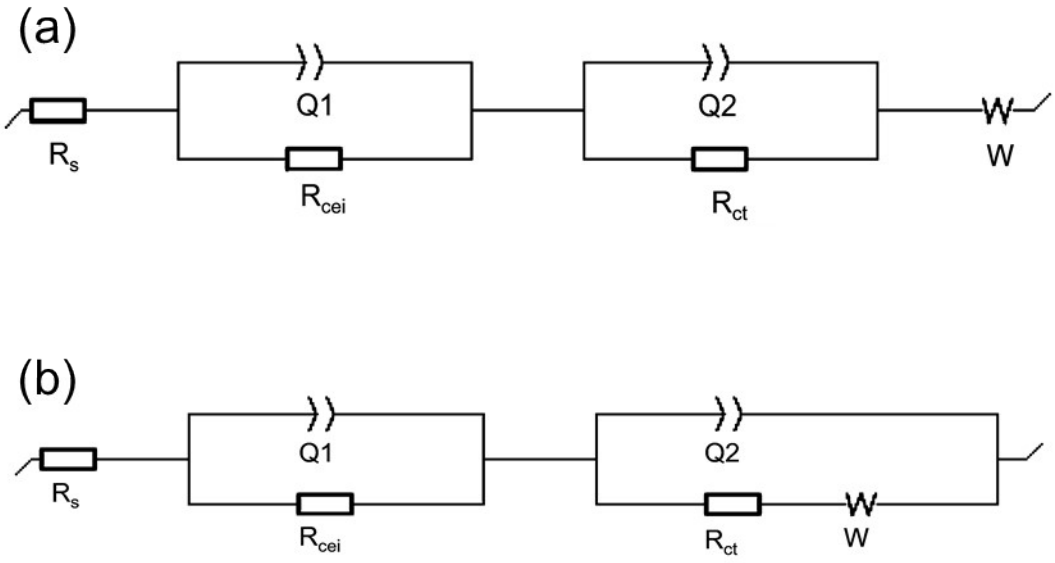


**Fig. S11** Equivalent circuit model for the fitting of Nyquist plot at (a) after 3rd cycle and (b) after 250$^{th}$ cycle.

**References :**


1 X. Zhang, B. Peng, L. Zhao, G. Wan, F. Wang, S. Zeng, H. Zhang, J. Ding and G. Zhang, *ACS Appl. Mater. Interfaces*, 2022, **14**, 16204–16213.
2 K. Tang, X. Yu, J. Sun, H. Li and X. Huang, *Electrochimica Acta*, 2011, **56**, 4869–4875.
3 Y. Cui, X. Zhao and R. Guo, *Electrochimica Acta*, 2010, **55**, 922–926.
4 C. Hong, Q. Leng, J. Zhu, S. Zheng, H. He, Y. Li, R. Liu, J. Wan and Y. Yang, *J. Mater. Chem. A*, 2020, **8**, 8540–8547.
5 K. Märker, P. J. Reeves, C. Xu, K. J. Griffith and C. P. Grey, *Chem. Mater.*, 2019, **31**, 2545–2554.
6 H.-J. Noh, S. Youn, C. S. Yoon and Y.-K. Sun, *J. Power Sources*, 2013, **233**, 121–130.